Response of Primary Human Airway Epithelial Cells to Influenza Infection: A Quantitative Proteomic Study

Andrea L. Kroeker,[†,‡,§] Peyman Ezzati,[‡] Andrew J. Halayko,[†,§] and Kevin M. Coombs*[,†,‡,§,‖]

[†]Manitoba Institute of Child Health and [‡]Manitoba Center for Proteomics and Systems Biology, John Buhler Research Center University of Manitoba, Winnipeg, Canada R3E 3P4

[§]Department of Physiology and [‖]Department of Medical Microbiology, Faculty of Medicine, University of Manitoba, Winnipeg, Canada R3E 0J9

S *Supporting Information*

ABSTRACT: Influenza A virus exerts a large health burden during both yearly epidemics and global pandemics. However, designing effective vaccine and treatment options has proven difficult since the virus evolves rapidly. Therefore, it may be beneficial to identify *host* proteins associated with viral infection and replication to establish potential new antiviral targets. We have previously measured host protein responses in continuously cultured A549 cells infected with mouse-adapted virus strain A/PR/8/34(H1N1; PR8). We here identify and measure host proteins differentially regulated in more relevant primary human bronchial airway epithelial (HBAE) cells. A total of 3740 cytosolic HBAE proteins were identified by 2D LC−MS/MS, of which 52 were up-regulated ≥2-fold and 41 were down-regulated ≥2-fold after PR8 infection. Up-regulated HBAE proteins clustered primarily into interferon signaling, other host defense processes, and molecular transport, whereas down-regulated proteins were associated with cell death signaling pathways, cell adhesion and motility, and lipid metabolism. Comparison to influenza-infected A549 cells indicated some common influenza-induced host cell alterations, including defense response, molecular transport proteins, and cell adhesion. However, HBAE-specific alterations consisted of interferon and cell death signaling. These data point to important differences between influenza replication in continuous and primary cell lines and/or alveolar and bronchial epithelial cells.

KEYWORDS: *Influenza virus, Primary cells, Quantitative proteomics, Host cell response, SILAC*

■ INTRODUCTION

Influenza A virus (IAV), a member of the Orthomyxoviridae family, is an enveloped, single-stranded RNA virus with a genome of 8 negative-sense segments, with most encoding a single gene. These eight segments give rise to 10 or 11 distinct proteins depending on the strain (NA, HA, NS1, NS2/NEP, M1, M2, NP, PA, PB1, PB1-F2, and PB2),[1] and these have been shown to interact extensively with each other and with host cell proteins throughout the virus lifecycle.[2] Some interactions elicit

alterations in the host proteome, as exemplified by the virus's ability to both induce and evade a host immune response,[3] to influence autophagy and apoptosis,[4−6] and to increase viral protein synthesis while shutting down host protein synthesis.[7] Numerous host proteins may also be important for influenza replication, as recently shown in whole genome siRNA screens that identified 100 genes in Drosophila,[8] 120 genes in U2OS cells,[9] as well as 295 genes[10] and 287 genes[11] in the A549 human carcinoma lung cell line.

Current anti-influenza therapies consist of only two classes of treatments, and these each target a viral protein: zanamivir and oseltamivir are neuraminidase inhibitors, while amantidine and rimantidine target the M2 protein. Recent and currently circulating strains from the 2010−2011 season have remained susceptible to M2 inhibitors; however, resistance to neuraminidase inhibitors is emerging (www.cdc.gov/flu/weekly/). Thus, new targets for which resistance will not quickly be developed are needed, and host cell proteins essential for viral replication represent one option.[12]

Studying virus−host interactions is increasingly reliant on quantitative proteomic techniques such as 2D-DIGE, isotope-encoded affinity tag (ICAT), and stable isotope labeling of amino acids in cell culture (SILAC). For example, SILAC profiling was used to determine differences in expression between HIV- and mock-infected T-cells[13] and the response of several host cell types to hepatitis C infection.[14,15] Quantitative proteomics has also been applied to influenza−host interactions, including several studies probing primary macrophages with iTRAQ[16] and 2DIGE-MS/MS[17] and multiple studies using similar techniques in continuous epithelial cell lines such as AGS,[18] MDCK,[19−21] A549,[22] and Calu-3 cells.[23] Several genomic and proteomic studies have also been carried out in influenza-infected macaques.[24−26] A novel aspect of the current study is the use of more relevant human primary bronchial epithelial cells, a model that more closely mimics *in vivo* infection conditions. It has been shown that the response to influenza depends not only on the viral strain[27] but also the host species, cell type and location in the lung,[28] and the state of cell differentiation.[29] While the effect of these different parameters have been characterized in part by measuring secreted cytokines[30] and the kinetics of viral replication,[27] very little is known about differences in host−virus interactions between different host cell types. Similarly, few studies have compared the effect of IAV infection in continuous and primary cell lines of specific cell types. Therefore, it is important to extend our previous SILAC studies using continuous human lung A549 cells, a type II alveolar epithelial cell, to primary human tracheobronchial airway epithelial (HBAE) cells to compare pathways affected by influenza replication, and identify pathophysiologically relevant responses.

■ EXPERIMENTAL PROCEDURES

Cells and Viruses

Viruses. Influenza virus strain A/PR/8/34 (H1N1; PR8), an attenuated mouse-adapted strain, was grown in embryonated hens' eggs from laboratory stocks, after which chorioallantoic fluid was harvested, aliquoted, and titered in MDCK cells by standard procedures.[22]

Cells and Media. Primary normal human broncho-tracheal epithelial cells were obtained from "healthy donors" by Lonza Inc. and were certified as mycoplasma-, HIV-, HBV-, and HCV-negative. Notably, these cells were capable of >10 cell doublings, which made the six doublings needed for SILAC labeling

possible. Cells were cultured in bronchial epithelial growth media (BEGM, Lonza Inc.), which consists of bronchial epithelial basal media (BEBM, Lonza Inc.) supplemented with SingleQuots (Lonza Inc.) containing bovine pituitary extract, hydrocortisone, hEGF, epinephrine, transferrin, insulin, retinoic acid, triiodothyronine, and gentamicin-1000. Cells were maintained as monolayers in 10% CO_2 at 37 °C and passaged by trypsinization at 80−90% confluence. For SILAC labeling, cells were grown in SILAC media that consisted of arginine- and lysine-free BEGM supplemented with either C12 ("light") or C13 ("heavy") lysine (29 mg/L) (mass difference of 6.0 Da) and C12/N14 ("light") or C13/N15 ("heavy") arginine (348 mg/L) (mass difference of 10.0 Da). Light amino acid containing media were prepared from regular stock powder (Sigma, St, Louis MO), and heavy amino acids were obtained from the SILAC Phosphoprotein Identification and Quantification Kit (Invitrogen Canada Inc.; Burlington, Ontario). Separate SILAC labeling and infection experiments were performed four times.

Infection. For SILAC experiments, all cells were grown in a pair of T75 flasks in SILAC media for six cell doublings; after the sixth cell doubling, cells were allowed to reach near confluency. In three replicates C12/N14-light cells were infected with egg-grown PR8 virus that was diluted in gel saline to achieve a multiplicity of infection (MOI) of 7 plaque forming units (PFU) per cell. An equivalent number of C13/N15-heavy cells were mock infected as a control using only gel saline. Previous studies indicate the small amount of egg protein makes no significant measurable contribution to results or conclusions.[22] Label swapping was performed for the fourth replicate; the C13/N15 heavy cells were infected, and the C12/N14 light cells were mock infected. For all other infections, cells were grown to near confluency and infected at various MOIs as indicated. In order to synchronize infections, virus- and mock-infected cells were placed at 4 °C for the 1 h virus adsorption, after which inoculum was removed and cells were overlaid with appropriate prewarmed light or heavy SILAC media. Infected and mock-infected cell cultures were then kept at 37 °C until analysis of viral replication and host protein expression. Efficiency of infection was always confirmed by a standard plaque assay as described previously.[22]

Isolation of Cytosolic Proteins

Twenty-four hours postinfection, cells grown in C12/N14-light or C13/N15-heavy BEGM were collected by brief trypsinization and counted, and then equivalent numbers (roughly 3 × 10^6 cells) of each group were mixed together. To verify infection status of each culture, aliquots of all separate cultures were saved for virus titration by plaque assay as mentioned above. Mixed cells were washed 3 times in >50 volumes of ice-cold phosphate-buffered saline (PBS) and lysed for cytosolic proteins by adding NP-40 buffer (10 mM TrisHCl pH 7.4, 3 mM $CaCl_2$, 2 mM $MgCl_2$, 0.5% NP-40, 1.1 μM pepstatin A) to the cells and incubating them for 30 min on ice. Nuclei were pelleted at 5000 × *g* for 10 min and the supernatant was saved as "cytosol". Both fractions were frozen at −80 °C until further processing.

Protein Digestion

Protein content in the cytosolic fractions were measured using a Protein Assay Kit (Biorad) and bovine serum albumin standards. Three hundred micrograms of each was reduced, to which 6× the volume of 100 mM ammonium bicarbonate was added. Then 100 mM dithiothreitol (DTT) in 100 mM ammonium bicarbonate was added to the peptide mixture, and samples were incubated for 45 min at 60 °C. Iodoacetic acid (500 mM in

100 mM ammonium bicarbonate) was added to each tube for alkylation, and the tubes were incubated for a further 30 min (room temperature, in the dark). Finally, 100 mM DTT was added to quench the excess iodoacetic acid. Samples were digested overnight at 37 °C with 6 μg of sequencing grade trypsin (Promega, Madison, WI) and then stored at −80 °C until further processing.

2D LC−MS/MS and Peptide Identification

Peptide fractionation was carried out using a 2D RP (reversed-phase) high pH−RP low pH peptide system as described previously.[31] In short, lyophilized tryptic digests were dissolved in 200 μL of 20 mM ammonium formate pH 10 (buffer A), injected onto a 1 × 100 mm XTerra (Waters, Milford, MA) column and fractionated using a 0.67% acetonitrile per minute linear gradient (Agilent 1100 Series HPLC system, Agilent Technologies, Wilmington, DE) at a 150 μL/min flow rate. Sixty 1-min fractions were collected and concatenated using procedures described elsewhere;[31,32] the last 30 fractions were combined with the first 30 fractions in sequential order (i.e., no. 1 with no. 31; no. 2 with no. 32, etc.). Combined fractions were vacuum-dried and redissolved for the second dimension RP separation (0.1% formic acid in water). The second dimension was run on a splitless nanoflow Tempo LC system (Eksigent, Dublin, CA) with 20 μL sample injection via a 300 μm 5 mm PepMap100 precolumn (Dionex, Sunnyvale, CA) and a 100 μm × 200 mm analytical column packed with 5 μm Luna C18(2) (Phenomenex, Torrance, CA). Both eluents A (water) and B (acetonitrile) contained 0.1% formic acid as an ion-pairing modifier. A 0.33% acetonitrile per minute linear gradient (0−30% B) was used for peptide elution, providing a total 2-h run time per fraction in the second dimension.

A QStar Elite mass spectrometer (Applied Biosystems, Foster City, CA) was used in a data-dependent MS/MS acquisition mode. One-second survey MS spectra were collected (m/z 400−1500) followed by MS/MS measurements on the 3 most intense parent ions (80 counts/s threshold, +2 to +4 charge state, m/z 100−1500 mass range for MS/MS), using the manufacturer's "smart exit" (spectral quality 5) settings. Previously targeted parent ions were excluded from repetitive MS/MS acquisition for 60 s (50 mDa mass tolerance). Spectra were identified using Analyst QS 2.0 (Applied Biosystems) software.

Protein Identification and Quantification

Thirty ".wiff" files from Analyst were submitted simultaneously to Protein Pilot 3.0 (Applied Biosystems) for relative quantification and protein identification using the Paragon algorithm as the search engine. Each MS/MS spectrum was searched against a database of human protein sequences (NCBInr, released March 2008, downloaded from ftp://ftp.ncbi.nih.gov/genomes/H_sapiens/protein/). The search parameters allowed for cysteine modification by iodoacetic acid and biological modifications programmed in the algorithm (i.e., phosphorylations, amidations, semitryptic fragments, etc.). The threshold for detecting proteins (unused protscore (confidence)) in the software was set to 2.0 to achieve 99% confidence, and identified proteins were grouped by the ProGroup algorithm (Applied Biosystems, Foster City, CA) to minimize redundancy. The bias correction option was used to correct for small pipetting errors. The protein sequence coverage was calculated using peptides identified with >95% confidence. A decoy database search strategy (NCBInr *Homo sapiens* with all protein sequences reversed) was also used to estimate the false discovery rate (FDR), defined as the percentage of reverse proteins identified against the total protein

identification. For our data, the estimated FDR was 0.56%, which is low compared to other studies and indicates a very high reliability of the proteins identified.[33]

For relative quantitation, only peptides unique for a given protein were considered, thus excluding those common to other isoforms or proteins of the same family. Proteins were identified on the basis of having at least one peptide with an ion score above 99% confidence. Among the identified peptides, some of them were excluded from the quantitative analysis for one of the following reasons: (a) The peaks corresponding to the SILAC labels were not detected. (b) The peptides were identified with low identification confidence (<1.0%). (c) Either the same peptide sequence was claimed by more than one protein or more than one peptide was fragmented at the same time because of shared MS/MS spectra. (d) The sum of the signal-to-noise ratio for all of the peak pairs was 6 for the peptide ratios.

Bioinformatics and Statistics

In order to compare multiple biological replicates, protein ratios within each replicate were converted to a z-score that allowed protein ratios to be normalized to the mean and standard deviation of its individual experiment.[22] Thus, a protein with a z-score >1.960σ indicates that protein's differential expression lies outside the 95% confidence level, 2.576σ indicates 99% confidence, and 3.291σ indicates 99.9% confidence; z-scores >1.960 were considered significant. The weighted average z-score was then calculated for each protein found in multiple replicates.

Gi numbers of all significantly regulated proteins were submitted to and analyzed by the DAVID bioinformatic suite at the NIAID, version 6.7,[34,35] and gene ontologies were examined with the "FAT" and Panther databases. The gi numbers were also submitted to, and pathways constructed with, Ingenuity Pathway Analysis software (IPA).

Western Blotting

Mock- and influenza-infected HBAE cells were scraped into cold PBS at 24 hpi, pelleted at 5000 × g for 5 min, and lysed with lysis buffer (20 mM Tris pH 7.5, 100 mM NaCl, 0.5% NP-40, 0.5 mM EDTA, 1× antiprotease cocktail (Pierce), 1× phosphatase inhibitor cocktail (Pierce)). Forty micrograms of protein was loaded per lane into SDS-PAGE gels, separated, and transferred to nitrocellulose membranes. Membranes were probed with primary antibodies for viral NP (in-house antibody), viral NS-1 (in-house antibody), SamD9 (Sigma), IFIT1 (Epitomics), E-cadherin (Cell Signaling), GLG1 (Sigma), ISG15 (Rockland), MxB (Santa Cruz), RSAD2 (Abcam), STAT1 (Cell Signaling), β-tubulin (Cell Signaling), PPIA (Epitomics), OASL (Epitomics), β-actin (Sigma), and GAPDH (Santa Cruz) and rabbit HRP-conjugated secondary antibodies. Bands were detected with ECL (Amersham) and the AlphaInnotech FluorChemQ MultiImage III instrument, quantitated using AlphaEase software and virus-to-mock ratios reported without normalization.

Microscopy

HBAE cells were grown to 80% confluence on 25 mm coverslips and infected or mock-infected at MOI = 7. Mock and 0, 12, and 24 h infected cells were fixed in 3% paraformaldehyde for 15 min, permeabilized with 0.3% Triton-X100 in 3% paraformaldehyde for 15 min, and blocked with 1% BSA in PBS. Cells were treated with a primary antibody for NP (made in-house) and a Cy3-conjugated rabbit secondary antibody (Jackson Immuno Research); all antibodies were diluted in 1% BSA and PBS. Coverslips were then mounted onto slides using DAPI-Prolong Gold Antifade, dried, and sealed. Fluorescent images were
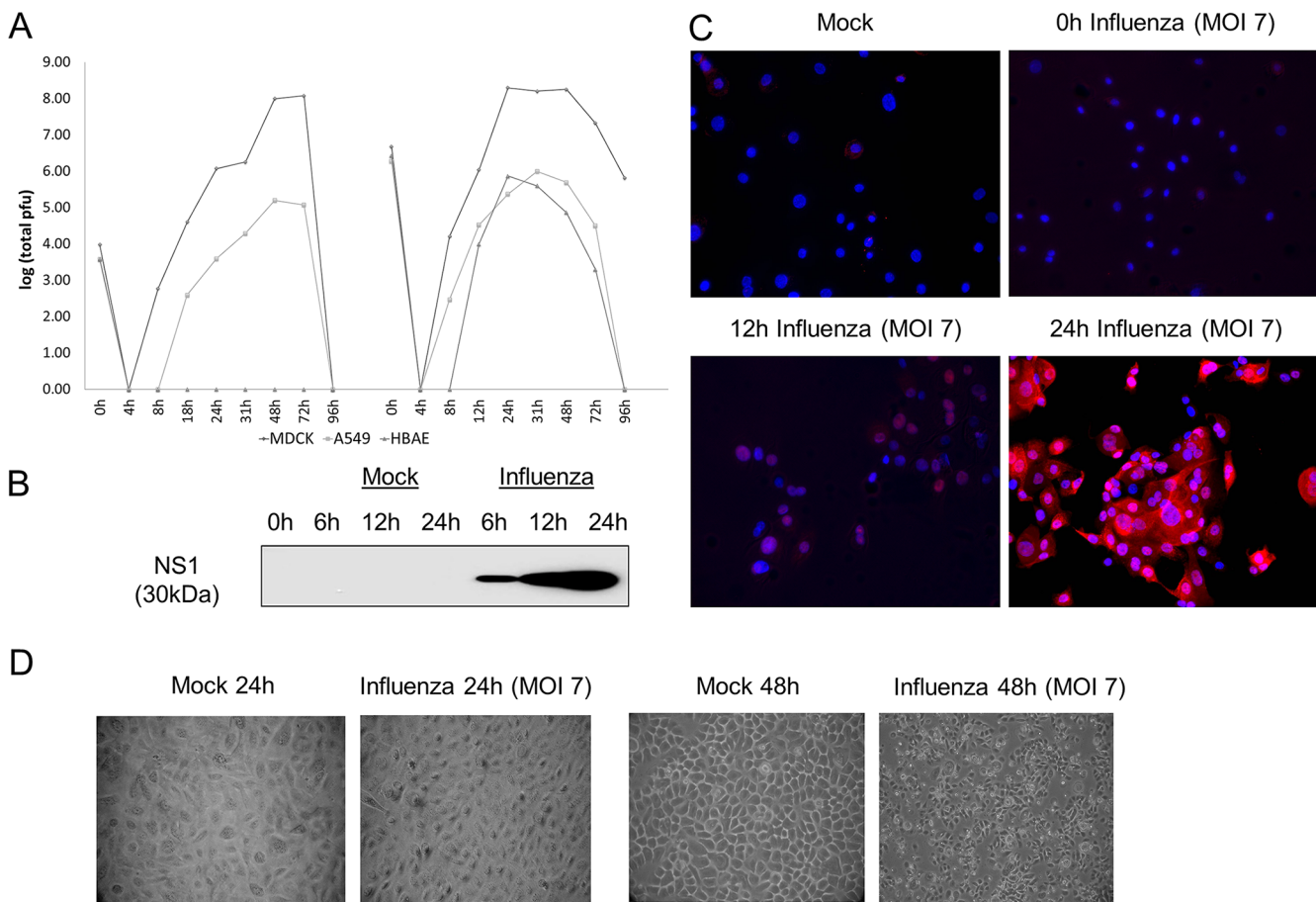
Figure 1. Active viral replication in HBAE. (A) HBAE, A549, and MDCK cells were infected at MOI = 0.01 (left) and 7 (right) PFU/cell to monitor and compare efficiency of infectious progeny virus production. Supernatants were collected and titered for progeny virus production by standard plaque assay at indicated time points. (B) HBAE cells were infected with influenza A/PR/8/34 at MOI = 7 PFU/cell, and protein lysates were assayed for accumulation of viral NS-1 protein at 6, 12, and 24 h post infection by Western blotting. (C) HBAE cells were infected for 0, 12, and 24 h at MOI = 7 PFU/cell. After fixation, the percentage of cells infected by virus was shown using immunocytochemistry for the viral nucleoprotein. NP = red; nuclei = blue. (D) Phase-contrast images of HBAE cells at 24 and 48 h post infection and mock infection.

obtained using a computer-controlled Olympus IX70 microscope (20X objective) equipped with CCD camera and NIS-Element software.

■ RESULTS

A/PR/8/34 Replicates in Undifferentiated Primary HBAE Cells

Actively proliferating primary epithelial cell cultures are not commonly used for influenza studies; thus, we initially determined optimal conditions for influenza replication in nondifferentiated HBAE. A low (0.01) and a high (7) MOI were initially chosen to measure the amount of infectious progeny virus released into the supernatant over time. At the low MOI, viral replication was most efficient in MDCK cells, as peak titers reached almost 10^8 PFU/mL by 48 hpi, whereas maximum titers of 10^5 PFU/mL were attained by 48 hpi in A549 cells and no detectable virus was recovered from HBAE cells (Figure 1a). At MOI = 7, MDCK and A549 cells reached similar peak titers but at earlier time points, 24 and 31 hpi, respectively; HBAE produced detectable virus by 12 hpi and reached a maximum titer of 10^5 PFU/mL by 24 hpi (Figure 1b). Influenza replication in HBAE at MOI = 7 was further confirmed by Western blotting for the viral non-structural-1 protein (NS1), which is expressed only during active viral replication. NS1 was clearly expressed in

HBAE cells by 6 hpi and increased in abundance at both 12 and 24 hpi (Figure 1b). Additionally, we found that an MOI = 7 was sufficient to demonstrate active and productive infection in approximately 50% of cells by 12 hpi, while >95% of cells demonstrated productive infection by 24 hpi (Figure 1c). For SILAC experiments we therefore chose to study cells 24 h after infection to maximize the amount of time for cellular proteomic changes to occur while retaining active virus replication and minimizing any cytopathic effect (Figure 1d). These data collectively indicate that primary HBAE cells support influenza virus replication. In addition, to verify that HBAE cells could be labeled, we analyzed only heavy-labeled cells using LC−MS/MS and ProteinPilot.[36−38] Using the data from ProteinPilot, we determined that 91% of all peptides contained the "C13-label" modification (Supplementary Figure 1). In addition, H:L ratios were reported for each peptide. The C13-containing peptides were highly enriched for high H:L ratios; 66% of these peptides had an H:L ratio >9 (>90% incorporation), and 92% had an H:L ratio >2 (>67% incorporation). In contrast, the peptides that did not contain a C13 label were enriched for peptides with low H:L ratios, e.g., 75% of these peptides had an H:L ratio <1 (<50% incorporation), and virtually all unlabeled peptides belonged to keratins. Therefore, we concluded that the six HBAE cell doublings were sufficient to label the cell proteome.
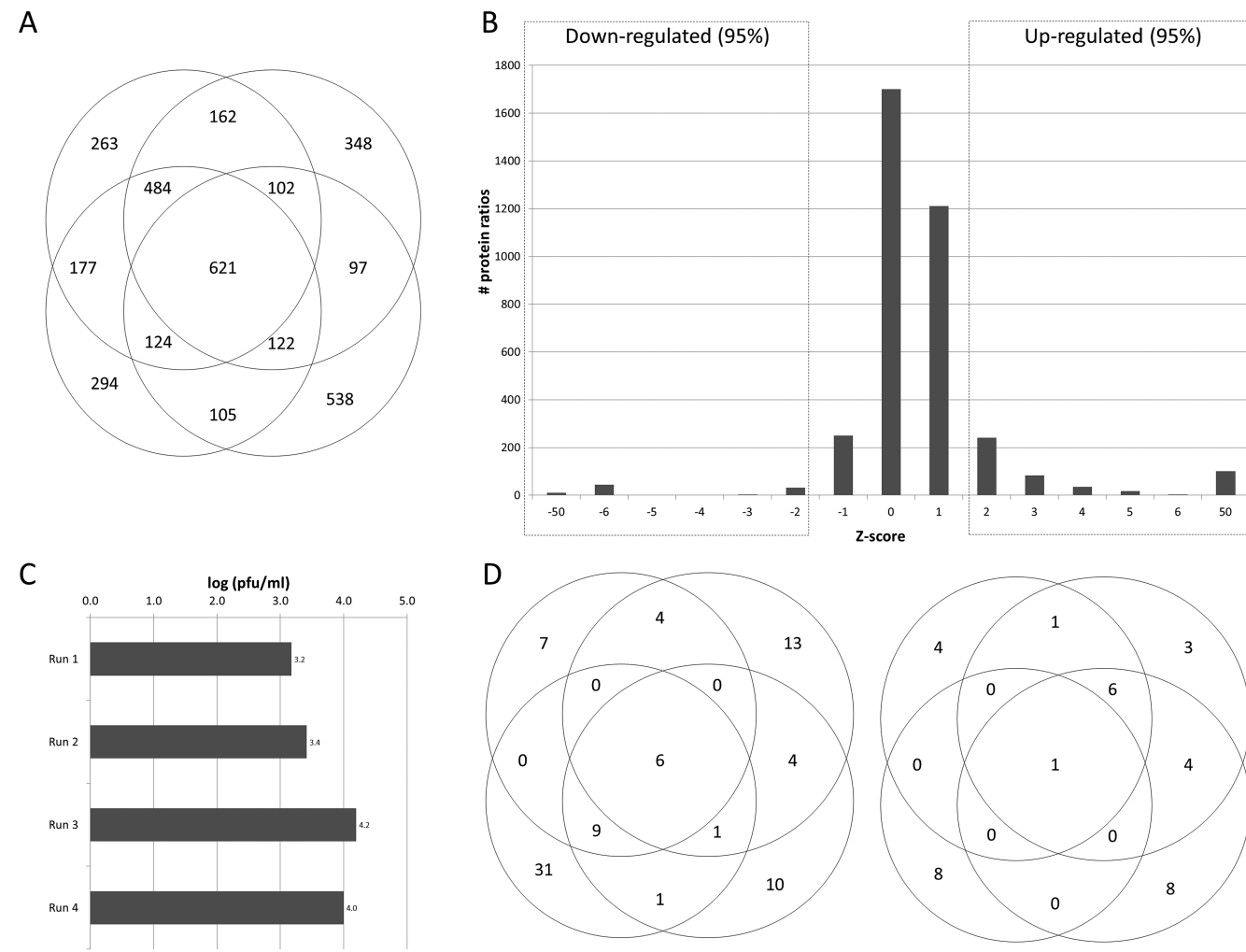
Figure 2. Distributions of total, up-regulated, and down-regulated proteins identified. (A) A total of 3740 proteins were identified from four separate biological replicates; 30% of all proteins were found in every run, 53% were found in two or more runs, and 46% were unique to each run. (B) Up- and down-regulated proteins were determined statistically using a frequency distribution curve. In order to compare the four replicate runs, infected:mock ratios for each run were normalized by converting them to z-scores, a measure of deviation from the average. Therefore, positive values represent proteins that are up-regulated in virus-infected cells, and negative values represent down-regulated proteins. To determine which proteins are significantly altered in abundance we used different confidence intervals as indicated. Most proteins were not significantly altered (z-score between −1 and 1); however, a small subset of proteins were strongly up- or down-regulated (z-score >1.96 and <−1.96, respectively; p-value <0.05). Only one of the replicates is shown for clarity. (C) After SILAC-labeled HBAE cells were infected for 24 hpi, the supernatant was collected and titered by plaque assay to demonstrate that the cell monolayer had been infected and had productively produced progeny virus. (D) The number of up- and down-regulated protein pairs identified in each trial at a confidence level of 95% (z-score >1.96). Specific peptides identified, measured, and used to measure up-regulated and down-regulated proteins are listed in Supplementary Table 3.

SILAC Identified 3740 Unique Cytosolic HBAE Proteins

We performed four separate replicate experiments using primary human bronchial epithelial cell cultures from the same donor in which the light-labeled culture was infected in three replicates and the heavy-labeled culture was infected for the fourth replicate. This allowed us to demonstrate that the heavy isotopes had no effect on the virus replication. Several proteins were found significantly up-regulated in the light-labeled infections but significantly down-regulated in the heavy-labeled infection. These proteins, which therefore probably represent contaminants, include several keratin species (1, 2, 9), dermcidin, transferrin, thyroid hormone receptor associate protein 3, and nipsnap2 and were excluded from subsequent analysis. Overall, a total of 3740 unique cytoplasmic proteins were detected and quantified; 2282 (61%) of these proteins were detected in 2 or more replicates, 1453 (39%) were found in 3 or more replicates, and 621 (17%) were common to all four replicates (Figure 2a). As these

proteins were identified using a human database and rely upon the presence of these proteins in both cultures, no viral proteins were identified during mass spectrometry. To confirm that the samples were infected, supernatants were titered for progeny virus using a standard plaque assay on MDCK cells (Figure 2b).

Comparing the abundance of proteins in infected cultures to uninfected cultures revealed that 97% of all proteins were present in approximately equal amounts (near a 1:1 ratio), thus indicating that IAV infection does not alter the expression level of most proteins in host cells. To determine cutoff values for identifying significantly up- and down-regulated proteins, ratios for infected:uninfected in each trial were first converted to z-scores to normalize each run to its own mean and standard deviation, thus allowing us to compare multiple runs. By converting an average z-score back into an average protein ratio, we determined that a z-score of 1.96 (95% confidence interval) corresponded to a 2-fold change. Similarly, z-scores of 2.58 (99% confidence interval) corresponded to a protein ratio change of 2.5-fold and z-scores of

Table 1. HBAE Proteins Increased >95% Confidence[a]

gi accession	symbol	gene name	virus/mock protein ratio					no. of peptides used for identification			
			run 1	run 2	run 3	run 4	ratio avg	run 1	run 2	run 3	run 4
		Cytosolic Proteins Detected More than Once									
gil6650772	PRO1400	PRO1400	100.0		100.0		100.0	18		17	
gil33286420	PKM2	pyruvate kinase 3 isoform 2		100.0	100.0		100.0		81	70	
gil5732237	MLYCD	malonyl coenzyme A decarboxylase	100.0	100.0			100.0	1	1		
gil11321577	OASL	2′-5′-oligoadenylate synthetase-like isoform a		10.0	24.5		17.2		1	1	
gil12654159	IFITM1	Interferon induced transmembrane protein 1 (9−27)	20.2	100.0			20.2	3	3		
gil19923667	RSAD2	Radical S-adenosyl methionine domain containing 2	20.9	13.9	10.0	100.0	14.9	7	13	8	1
gil55958476; gil13436398	IFIT3/4	interferon-induced protein with tetratricopeptide repeats 3/4	3.2	8.5	30.8	1.6	11.0	8	8	11	4
gil52694752	GPNMB	glycoprotein (transmembrane) nmb isoform a precursor	4.1	10.7			7.4	1	1		
gil2996631; gil7717386	MX2	MX2	13.7	8.1	100.0	2.7	8.2	2	3	3	3
gil21751732; gil7717387	MX1	Myxovirus resistance 1, interferon inducible protein p78	7.7	3.7	10.9	4.7	6.7	3	3	8	4
gil5834273	HMGA1	high mobility group protein-R	19.7	2.1			10.9	2	1		
gil54697154	MMP1	matrix metalloproteinase 1 (interstitial collagenase)	3.5	10.1	4.5		6.0	2	4	1	
gil34192824; gil55958474	IFIT2	Interferon-induced protein with tetratricopeptide repeats 2	7.3	5.5	8.8	2.5	6.0	7	5	11	
gil49574526	IFIT1	interferon-induced protein with tetratricopeptide repeats 1	6.6	3.2	4.9	4.0	4.7	6	6	10	3
gil14550514; gil4826774	ISG15	ISG15 ubiquitin-like modifier	3.6	3.4	2.7	10.8	5.1	3	3	3	4
gil34783544	LGALS7	LGALS7 protein	4.8	3.6	1.6		3.3	1	7	1	
gil297097; gil452647	HLA-B/C	HLA-C α chain	3.8		2.4		3.1	10		10	
gil56204179	GBP1	Guanylate binding protein 1, interferon-inducible, 67 kDa		100.0		2.9	2.9				
gil39794319	SPBN	Suprabasin	2.5	3.0			2.8	1	1		
gil14602986	ACTC1	Actin, α, cardiac muscle	1.6	4.6	100.0		3.1	44	52	54	
gil54673572	LYRM7	Hypothetical protein LOC90624	2.9	4.1	1.4		2.8	2	2	3	
gil4886493	SAMHD1	SAM domain and HD domain 1		2.0	3.0		2.5		2	1	
gil13937981; gil48145531	PPIA	Peptidylprolyl isomerase A (cyclophilin A)		2.3	2.1		2.2		23	22	
gil8922707	TMEM34	transmembrane protein 34	3.0	1.8			2.4	1	2		
gil2459624	TLR2	Toll-like receptor 2	1.6	2.5	2.6		2.2	1	4	1	
		Cytosolic Proteins Detected Only Once									
gil56203096	ACOT7	brain acyl-CoA hydrolase (BACH)	100.0				100.0	8			
gil15079723	DBNL	Drebrin-like	100.0				100.0	6			
gil38013966	TKT	TKT protein		100.0			100.0		56		
gil12053853	METTL9	Methyltransferase like 9		100.0			100.0		2		
gil14549669	COG3	vesicle docking protein SEC34			100.0		100.0			2	
gil485388	EIF4	eukaryotic initiation factor 4				100.0	100.0				9
gil457262	YBX1	Y box binding protein 1				100.0	100.0				4
gil55660909	SEC23B	Sec23 homologue B (S. cerevisiae)				100.0	10.00				4
gil415849	ADSS	adenylosuccinate synthetase				100.0	100.0				3
gil182642	–	rapamycin-binding protein				100.0	100.0				2
gil535179	BCAM	basal cell adhesion molecule (receptor for laminin)				100.0	100.0				2
gil5726629	SNX12	sorting nexin 12				100.0	100.0				2
gil16924221	ZNF259	Zinc finger protein 259				100.0	100.0				2
gil32479340	HN1	hematological and neurological expressed 1				100.0	100.0				2
gil55743134	RPS6KA1	ribosomal protein S6 kinase, 90 kDa, polypeptide 1 isoform b				100.0	100.0				2
gil33316810	OEF1	OEF1				100.0	100.0				2
gil1552516	–	trypsinogen C	65.1				65.1	7			
gil11120626	TYR6	cationic trypsinogen	38.9				38.9	6			
gil7582292	eIF4A2	Eukaryotic translation initation factor 4, A2		12.1			12.1		7		
gil12001972	BOLA2	My016 protein			14.6		14.6			3	
gil48146353	HSPBP1	HSPA (heat shock 70 kDa) binding protein, cytoplasmic cochaperone 1				68.6	68.6				2
gil52545561	MTPAP	Mitochondrial poly(A) polymerase			9.7		9.7			2	
gil30511	HBD	delta globin	8.4				8.4	2			
gil1335273	NOMO1	pm5 protein	7.0				7.0	25			
gil18418633	HBB	mutant β-globin		5.4			5.4		2		
gil999893	–	Chain B, Triosephosphate Isomerase (Tim) (E.C.5.3.1.1) Complexed With 2-Phosphoglycolic Acid				12.9	12.9				22

Table 1. continued

gi accession	symbol	gene name	virus/mock protein ratio					no. of peptides used for identification			
			run 1	run 2	run 3	run 4	ratio avg	run 1	run 2	run 3	run 4
		Cytosolic Proteins Detected Only Once									
gil51476968	STAT1	Signal transducer and activator of transcription 1		3.9			3.9			7	
gil9955206	–	Chain B, Crystal Structure Of A Rac-Rhogdi Complex				8.4	8.4				2
gil7671655	TOMM34	translocase of outer mitochondrial membrane 34				7.8	7.8				2
gil41351087	CAD	Carbamoyl-phosphate synthetase 2, aspartate transcarbamylase, and dihydroorotase				7.5	7.5				5
gil24899174	SAMD9	Sterile α motif domain containing 9		2.9			2.9		4		
gil6573422	–	Chain D, Human Glyoxalase I Complexed With S–P–Nitrobenzyloxycarbonylglutathione				7.1	7.1				2
gil48145879	CTSH	CTSH		2.8			2.8		3		
gil55960299	GSN	gelsolin (amyloidosis, Finnish type)				6.6	6.6				4
gil38174528	PPP4R1	Protein phosphatase 4, regulatory subunit 1				6.5	6.5				2
gil55663625	GOT1	glutamic-oxaloacetic transaminase 1, soluble (aspartate aminotransferase 1)				6.1	6.1				5
gil182518	FTL	ferritin light subunit				5.9	5.9				2
gil1843434	TXNRD1	thioredoxin reductase 1				5.5	5.5				4
gil15418999	ANTXR2	capillary morphogenesis protein-2		2.5			2.5		2		
gil56204739	HIST3H2A	histone 3, H2a		2.4			2.4		2		
gil4503445	TYMP	thymidine phosphorylase (endothelial growth factor)				4.9	4.9				3
gil40674605	CAPNS1	CAPNS1 protein		2.3			2.3		7		
gil30581141	PSME1	proteasome activator subunit 1 isoform 2		2.3			2.3		11		
gil3036787	HIST1H2BK	histone 1, H2bk		2.3			2.3		7		
gil12803167	NAP1L1	Nucleosome assembly protein 1-like 1				4.7	4.7				4
gil13623579	CLPB	caseinolytic peptidase B homologue (*E. coli*)		2.3			2.3		2		
gil15080241	PACSIN3	Protein kinase C and casein kinase substrate in neurons 3		2.2			2.2	7			
gil4507207	SRI	sorcin isoform a				4.5	4.5				2
gil544482	ALDH1A3	aldehyde dehydrogenase 6				4.3	4.3				17
gil12803089	NUTF2	Nuclear transport factor 2				4.3	4.3				2
gil55960474	ANXA7	annexin A7				4.3	4.3				7
gil51895905	STMN1	Stathmin1/oncoprotein 18				4.2	4.2				4
gil12654831	PGM3	Phosphoglucomutase 3				4.2	4.2				2
gil13623581	TXNDC17	Thioredoxin domain containing 17				4.1	4.1				3

a Ranked by average z-score.

3.29 (99.9% confidence interval) corresponded to a 3.0-fold change in protein ratio (Figure 2c). Further bioinformatic analyses were primarily performed with the 95% confidence data set but were also compared to more restricted data sets based on 99% and 99.9% confidence intervals (not shown).

Proteins that were identified with only a single peptide were excluded from our data set if they were detected in only a single run; however, any protein identified in multiple trials was included. We also excluded proteins from further analysis if they were not consistently up- or down-regulated between replicate runs. Some proteins identified in the current study were unaltered in at least one replicate and up- or down-regulated in other replicate(s). For these scenarios we grouped ratios into three groups: (a) z-scores −0.09 to 0.9 ("not altered"), (b) ±1.0 to 1.96 ("moderately altered"), or (c) greater than ±1.96 ("highly altered"). We then included only those proteins that had significant values (group c) in at least two runs or one of two runs; additionally, any trial with a nonsignificant value had to have that value still fall within the 80% confidence range (group b) to be considered. Outliers could be found at both the peptide and the protein level such that peptides and proteins that were found only in the virus or mock sample were labeled "9999" or "0000", respectively. We did not remove any outliers at the peptide level but found that they made up a very small percentage of the peptides in our lists of differentially regulated proteins (the details may be found in Supplementary Table 2) and removing them had minimal impact on the overall protein ratio.

For proteins that had a ratio of "9999" and "0" we arbitrarily assigned a z-score of 50 and −50, respectively. These outliers were not included in the statistical analysis but were reincorporated into data sets for further bioinformatic and biological analyses.

In summary, we used stringent parameters to generate a data set of proteins of interest based on 99% confidence in protein identification; protein identification based on 2 or more peptide pairs; 95% confidence interval for altered regulation; and the necessity for proteins to show consistent infected:unifected ratios. In this manner we identified 52 up-regulated proteins and 41 down-regulated proteins from PR8-infected primary HBAE cells (Figure 2c and listed in Tables 1 and 2). The identities, associated z-scores and protein percent coverage of the 52 up-regulated and 41 down-regulated proteins are listed in Supplementary Table 1, and the identities, confidences and other statistical parameters of the specific peptides used for quantitation are listed in Supplementary Table 2. Several of the up-regulated and nonregulated proteins that were identified in the SILAC analysis were confirmed by Western blotting (Figure 3), and most Western blot results confirmed SILAC-determined regulation status. Only one protein, PPIA, that was shown to be up-regulated in SILAC, was not validated using Western blotting. This may be caused by inherent differences in sampling (partially degraded proteins would not be measured by Western blot but their peptides would be detected by MS) or by inherent differences in the different methods' levels of sensitivity.

Table 2. HBAE Proteins Decreased >95% Confidence[a]

gi accession	symbol	gene name	virus/mock protein ratio					no. of peptides			
			run 1	run 2	run 3	run 4	ratio avg	run 1	run 2	run 3	run 4
Cytosolic Proteins Detected More than Once											
gi|56205024	PFDN4	PFDN4	0		0		0	2		2	
gi|10798851	FADS2	fatty acid desaturase 2		0.1	0.5		0.3		1	2	
gi|38511857	GLG1	Golgi apparatus protein 1	0.3	0.2	0.3	0.4	0.3	11	8	13	11
gi|1107687	FAT1	homologue of Drosophila Fat protein		0.4	0.3		0.3		6	7	
gi|14328083	FDFT1	Farnesyl-diphosphate farnesyltransferase 1	0.3	0.3	0.4		0.3	11	12	13	
gi|56206185	SPRR2D	small proline-rich protein 2D	0.6		0.2		0.4	6		2	
gi|55662663	COL12A1	collagen, type XII, α 1		0.3	0.4		0.4		1	2	
gi|8489095	TNFRSF10B	Fas-like protein precursor		0.4	0.4		0.4		4	4	
gi|40317626	THBS1	thrombospondin 1 precursor	0.4	0.3	0.5		0.4	50	63	55	
gi|28881898	F3	tissue factor	0.4	0.4	0.4		0.4	5	5	6	
gi|34364820; gi|16933542	FN1	Fibronectin 1	0.4	0.4			0.4	55	75		
gi|7243073	ADAMTS1	Metalloprotease with thrombospondin type 1 motif, 1	0.4	0.3	0.6		0.4	2	2	4	
gi|9971118	JAG1	JAG1	0.5		0.3		0.4	1		2	
gi|1945072	TNFRSF 10A	cytotoxic ligand TRAIL receptor	0.5		0.4		0.4	2		1	
gi|3282161	TGFBI	Transforming growth factor, β-induced, 68 kDa	0.5	0.4	0.4		0.4	2	2	2	
gi|54607033	INTB4	integrin β 4 isoform 3 precursor		0.4	0.4	0.5	0.5		49	43	36
gi|12274842	LAMA5	Laminin 5		0.5		0.5	0.5		7		4
gi|55662275	IGFR2	Insulin-like growth factor 2 receptor	0.5	0.4	0.6	0.6	0.5	16	15	17	14
gi|55960673	PTPRF	Protein tyrosine phosphatase, receptor type, F	0.7	0.5	0.6	0.4	0.5	1	3	3	4
gi|15080220	C1orf212	C1orf212 chromosome 1 open reading frame 212	0.7	0.4		0.6	0.6	2	1		2
gi|46020022	LAMA3	laminin α 3b chain	0.4			0.7	0.4	79			58
Cytosolic Proteins Detected Only Once											
gi|31979223	RPLP1	acidic ribosomal phosphoprotein P1	0				0	8			
gi|55957204	NUP50	Nucleoporin 50 kDa		0			0		2		
gi|13436176	FADS3	Fatty acid desaturase 3		0			0		2		
gi|55962101	EIF4G3	eukaryotic translation initiation factor 4 gamma, 3		0			0		2		
gi|18568105	RAB22	RAB22		0			0		2		
gi|2772927	TGOLN2	Trans-Golgi network protein 2		0.03			0.03		2		
gi|48775023	RELA	RELA protein			0.3		0.3				2
gi|7688699	RER1	Retention in endoplasmic reticulum homologue 1		0.3			0.3			3	
gi|52545861	TRAPPC9	Trafficking protein particle complex 9		0.4			0.4			3	
gi|14336424	MCAM	cell surface glycoprotein P1H12 precursor		0.4			0.4		3		
gi|6066280	CROT	peroxisomal carnitine octanoyltransferase		0.4			0.4		3		
gi|4505149	SERPINB7	serine (or cysteine) proteinase inhibitor, clade B (ovalbumin), member 7		0.4			0.4		2		
gi|7022598	DARS2	Aspartyl-tRNA synthetase 2, mitochondrial		0.4			0.4			3	
gi|16041779	SLC39A14	SLC39A14 protein		0.4			0.4			2	
gi|37537242	RNF149	Ring finger protein 149		0.5			0.5		2		
gi|34533080	SH3BP1	SH3-domain binding protein 1		0.5			0.5			3	
gi|48735299	SNRPA1	Small nuclear ribonucleoprotein polypeptide A'		0.4			0.4			3	
gi|13529266	PSMC6	Proteasome (prosome, macropain) 26S subunit, ATPase, 6		0.4			0.4			10	
gi|1825562	PDCD4	nuclear antigen H731		0.5			0.5	4			

[a]Ranked by average z-score.

Up-Regulated Proteins Are Associated with Host Cell Defense Responses, Endocytosis, and GTPase Activity

Gene ontology analyses using GO and Panther classification terms were determined for proteins that were up-regulated in response to influenza infection and compared at three different confidence intervals: 95% (z-score >1.96), 99% (z-score >2.58) and 99.9% (z-score >3.29) (Figure 4a). Additionally, canonical pathways and networks that were represented by influenza-altered proteins were constructed with IPA at the 95%, 99%, and 99.9% confidence intervals. Representative pathways and networks are shown only at the 95% interval. Approximately half of the proteins up-regulated in response to influenza infection in HBAE could be attributed to interferon and other known host cell defense responses. These proteins were identified by several gene ontology categories including defense response, immune response, response to virus and defense response to virus (Figure 4a). Collectively, these categories included proteins ISG15, RSAD2, MX1, MX2, IFIT1, IFIT2, IFIT3/4, IFITM1, SAMD9, SAMHD1, OASL, OAS3, TLR2, STAT1, GBP-1, and HLA-B/C. Pathway analyses also identified immune systems and interferon signaling (Figure 5, Supplementary Figure 2a). Proteins belonging to endocytic and
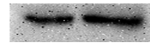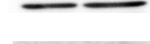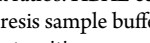
	Protein	kDa	Mock PR8	WB ratio	SILAC ratio
Up-regulated	NP	60		n.a.	*
	ISG15	18		n.a	5.12
	OASL	59		n.a.	17.23
	RSAD2	42		3.98 n.a.	14.91
	SAMD9	184		3.21	2.91
	IFIT1	55 50		1.00 n.a.	4.02
	MX2	72		40.00	10.90
	STAT1	80		1.80	3.89
Not regulated	GAPDH	37		1.13	1.10
	B-ACTIN	42		1.22	1.00
	B-TUB	76		1.22	1.50
Down-regulated	GLG1	135		0.05	0.33
	E-CAD	135		0.43	0.70
	PPIA	18		1.07	2.22

Figure 3. Western blotting was performed to confirm SILAC virus:mock ratios. HBAE cells were harvested and lysed with 0.5% NP-40 detergent, nuclei were removed, and cytosolic fractions were dissolved in SDS electrophoresis sample buffer, resolved in 8%, 10%, or 15% mini SDS-PAGE, transferred to PVDF, and probed with various antibodies. Bands were visualized and intensities were measured with an Alpha Innotech FluorChemQ MultiImage III instrument. Molecular weight standards are indicated at left and ratios of each protein (infected divided by mock-infected) are indicated for each protein at right, along with SILAC-measured ratios (far right). Western blot ratios for host proteins that were detected only in infected cells (undetectable in mock) are designated "n.a.". SILAC ratios are an average of the four replicate runs performed, and Western blotting ratios are from a single experiment in a different donor than was used for SILAC. Bands from Western blotting were quantitated using AlphaEase software and are reported without normalization. *: no viral proteins measured by SILAC because not present in mock-infected samples.

intracellular protein trafficking pathways were also indicated as up-regulated (Figure 4a) and included α-actin, MX1, MX2, and PPIA. Related canonical pathways that were identified by IPA include caveolar-mediated endocytosis, viral entry via endocytic pathways, and mechanisms of viral exit from host cells (Supplementary Figure 3b). A third category that was identified among influenza-up-regulated proteins was the presence of GTPase activity, which included proteins MX1, MX2, and GBP1 (Figure 4a).

Down-Regulated Proteins Are Associated with Cell Adhesion, Cell Death Signaling, and Lipid Metabolism

Many biological processes were represented among proteins down-regulated at the 95% confidence level. Notably, many of these are not cytosolic proteins but were mainly transmembrane (FADS2, ODZ2, FAT1, F3, GLG1, TNFRSF10A, JAG1, FDFT1, SLC16A2, TNFRSF10B) and extracellular matrix-related proteins (COL12A1, LAMA3, LAMA5, FN1, ADAMTS1, BIGH3) (Figure 4b). Cellular functions that were attributed to these proteins included cell adhesion (COL12A1, FAT1, FN1, GLG1, LAMA3, LAMA5) (Figure 4b) as well as signal transduction (ODZ2, collagen, FAT1, FN, F3, BIGH3, TNFRSF10A, TNFRSF10B, ADAMTS1) (Figure 4a).

TRAIL signaling, a process involved in inducing cell death, was also prominently identified (TNFRSF10A, TNFRSF10B) (Figures 4b and 5b, Supplementary Figures 2a and 3d). Third, several enzymes involved in lipid metabolic processes were consistently down-regulated including sterol metabolism (FDFT1) and fatty acid metabolism (FADS2, FADS3) (Figures 4b and 5b, Supplementary Figures 2b and 3d).

■ DISCUSSION

Our lab has previously used SILAC to study A549 alveolar epithelial cell host pathways that are altered in response to infection by influenza virus A/PR/8/34, a highly attenuated mouse-adapted strain of influenza virus.[22] We have now extended this work to include primary human airway epithelial cells, a model that is more closely related to the in vivo situation and that offers opportunity to assess the global relevance of proteomics data obtained using transformed human cell lines. Using a human database, we identified 3740 cytosolic HBAE protein pairs, of which only a small fraction was altered in response to A/PR/8/34 influenza infection. Proteins that were up- and down-regulated were determined statistically using different confidence intervals for which the 95% confidence
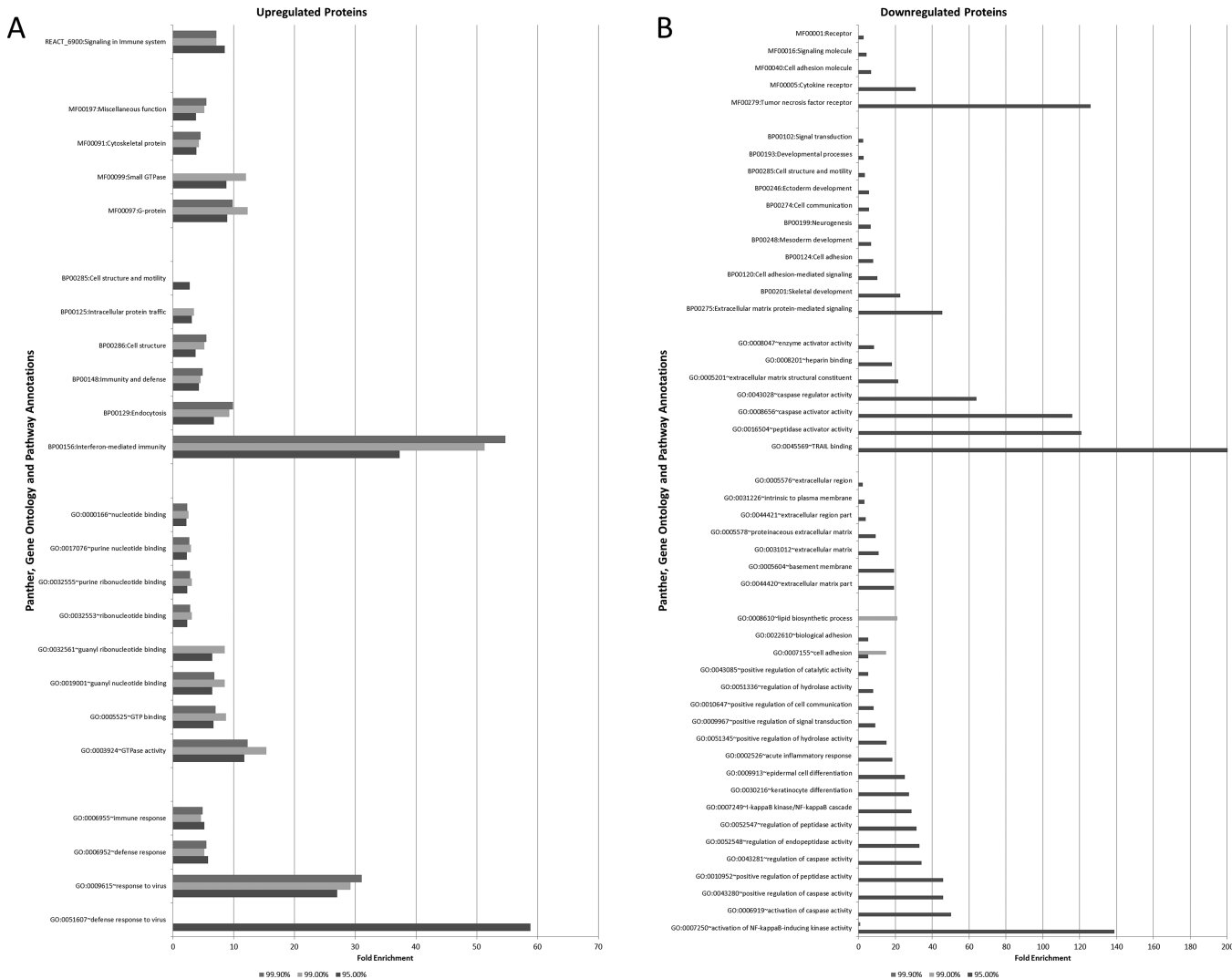
Figure 4. Gene ontology (GO) analysis of up- and down-regulated proteins. Lists of (A) up- and (B) down-regulated protein IDs were uploaded into DAVID separately and analyzed for enrichment of categories belonging to biological processes, cellular components, and molecular functions. Additionally, lists of proteins determined at different confidence intervals (95%, 99%, 99.9%) were compared.

interval corresponded to a 2-fold or more difference, the 99% limit to at least a 2.5-fold difference, and 99.9% confidence to a 3-fold or greater change. Since many previous studies have used either a 2-fold or 1.5-fold change in protein abundance to create data sets of infection-altered proteins,[14,15,22] the cutoff values used here are comparable. As viral proteins are not detected by human database searches, we titered the amount of virus secreted by our SILAC labeled cells at 24 hpi to ensure that viral infection and replication had been successful. It is worth noting that the maximum virus titers produced by HBAE vary from donor to donor. For example, the particular cells used in Figure 1a produced the highest titers we have observed in HBAE, whereas the cells used for the SILAC experiments (Figure 2c) produced considerably lower titers. However, despite these differences, we find robust viral protein expression in these cells from 6 to 72 hpi and can find comparable proteomic expression patterns among HBAE from different donors (data not shown).

The current study consists of the "cytoplasmic" cellular fraction, which includes all NP40 soluble components such as proteins of the cell membrane, cytoplasm, and cytoplasmic organelles, thereby excluding mainly nuclear proteins. We recognize that the nuclear sample is also an important component of the cell to analyze,

particularly because influenza virus replicates within the nucleus, and anticipate analyzing these fractions in future studies. However, the primary purpose of the present study was to compare HBAE results to A549 results,[22] and the later study had only been performed with the NP-40-soluble fraction.

Up-Regulated Processes

It is well documented that in many cell types interferon expression is a central cellular response to viral infection.[39−42] This is thought to be key in developing an antiviral state in both infected and neighboring noninfected cells to limit viral replication.[43] Consistent with this paradigm, in our current study up-regulated proteins in HBAE were chiefly enriched for host cell defense responses such as interferon (INF) and the JAK/STAT pathway (Figures 4a and 5a, Supplementary Figures 2a and 3a). Of note, influenza A can also antagonize interferon signaling via the viral NS-1 protein through multiple mechanisms including blocking host translation and sequestering viral RNA in order to prevent its detection by host pathogen recognition processes.[43,44] However, the extent of this inhibitory effect is strain-dependent,[43,45] and since the NS1 protein produced by the A/PR/8/34 influenza strain is generally thought to be a less
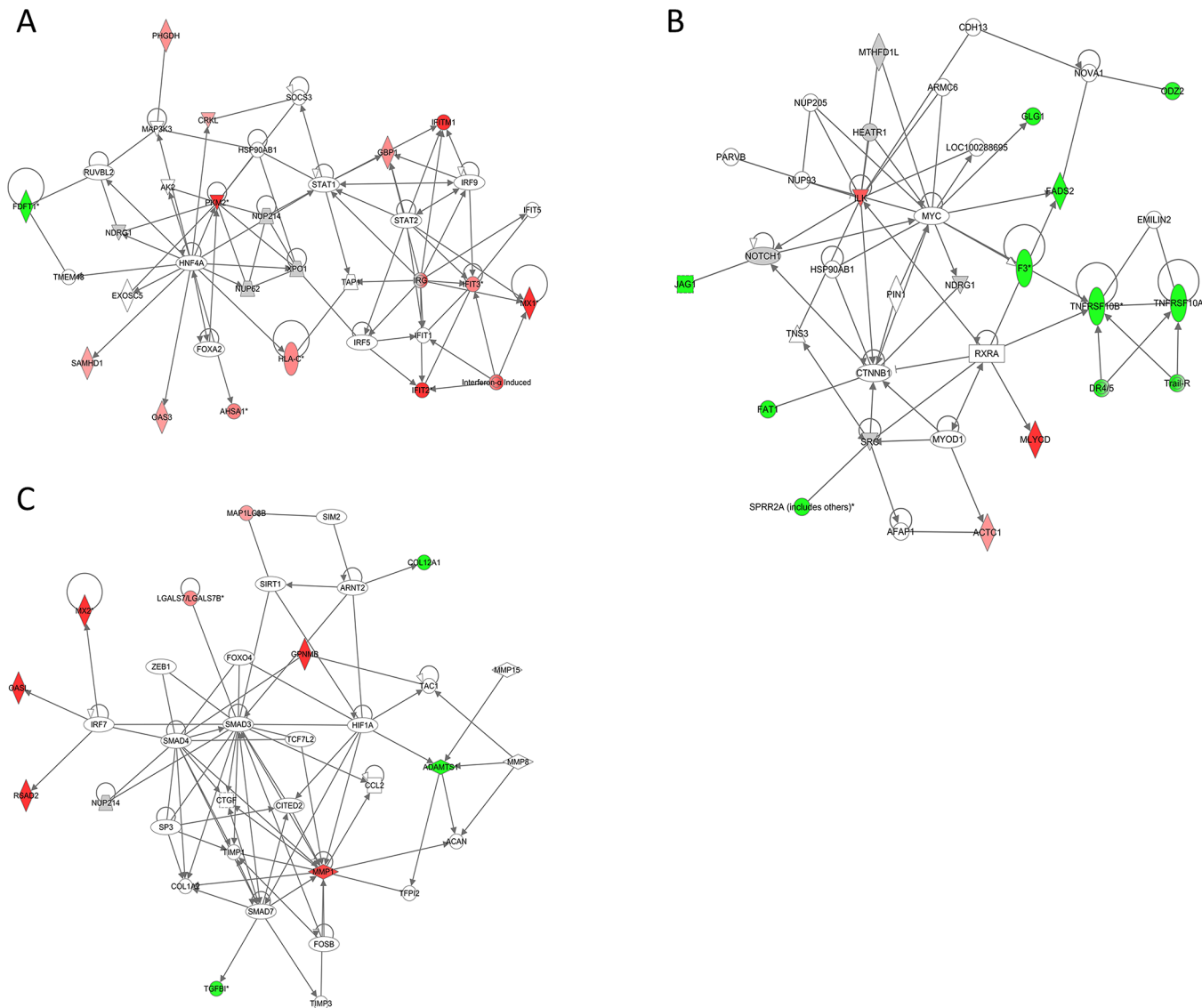
Figure 5. Interactions between up- and down-regulated proteins. Protein IDs and ratios from Tables 1 and 2 (95% confidence interval) were combined and imported into the Ingenuity Pathways Analysis (IPA) tool from which interacting pathways were constructed. Up- and down-regulated proteins are denoted in red and green, respectively; gray proteins indicate that they were detected in our study but not regulated; white proteins interact with many proteins in the network but were not detected in this study. Any known direct connections between these proteins are indicated by solid lines; indirect interactions are not shown here. Networks are titled (A) Infection, Gene Expression, Antimicrobial Processe; (B) Cancer, Dermatological Conditions, Cellular Development; and (C) Connective Tissues, Genetics, CV System Development and Function.

potent inhibitor of interferon production than other strains' NS1 protein,[43] this correlates well with our data.

Some of these findings were also unique to HBAE compared to our previous A549 study. Interestingly, neither GO nor IPA identified interferon signaling in PR8-infected A549 cells, whereas it was highly significant in HBAE cells (p-value = 0.001). In addition, while a few interferon-induced proteins (RSAD2, MX1, MX2, and ISG15) were highly up-regulated in both cell types, several (STAT1, RIG-I, SAMD9, SAMHD1, IFIT1, IFIT2, IFIT3) were highly up-regulated in HBAE but unaltered or undetected in A549. Indeed, we were able to confirm with Western blotting that cytosolic STAT1 abundance was increased in HBAE after influenza infection, whereas levels in A549 remained relatively unchanged. SamD9, a molecule downstream of STAT1, was more highly induced in HBAE than A549 after infection, whereas IFIT1 was detected only in HBAE after infection (Figure 6). This suggests that less interferon is produced by A549 than HBAE cells and

that this difference is dependent either on the cell type (A549 are alveolar epithelial in origin whereas HBAE are from airways) or properties of the cell line (i.e., primary versus transformed) rather than the virus strain. Notably, a difference in interferon signaling and production could explain the ability of A549, but not HBAE, to support replication of the PR8 virus when infected at a low MOI (0.01 PFU/cell). These observations provide rationale for future studies assessing the precise role(s) of interferon-associated proteins in preventing viral replication in primary epithelia and mechanisms that suppress this effect in transformed or alveolae-derived epithelial cells.

The interferon-induced proteins commonly up-regulated in both A549 and HBAE (RSAD2, MX1, MX2, and ISG15) were also identified in numerous other influenza studies. For example, myxovirus resistance host proteins Mx1 and Mx2 are up-regulated in a variety of cell models including MDCK[20] and A549[22,46] cells, as well as in vivo in studies with macaques.[26]

Protein	kDa	A549 Mock	A549 PR8	HBAE Mock	HBAE PR8	A549 WB ratio PR8/mock	HBAE WB ratio PR8/mock
NP	60						
STAT1	90					0.91 +/- 0.78	3.39 +/- 1.00
IFIT1	55					0.81 +/- 0.11	17.15 +/- 3.74
SAMD9	184					0.67 +/- 0.41	3.22 +/- 0.40
GAPDH	37						
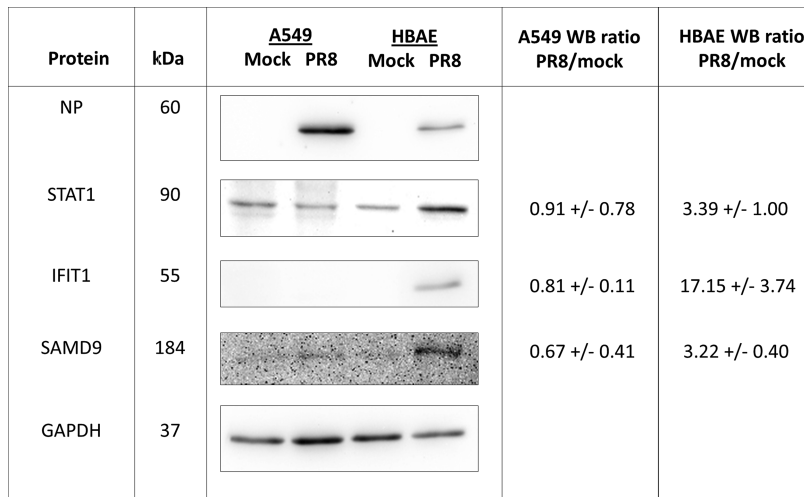
Figure 6. Comparison of JAK/STAT signaling molecule abundance in A549 and HBAE cells after influenza infection. Cells were harvested and lysed with 0.5% NP-40 detergent, nuclei were removed, and cytosolic fractions were dissolved in SDS electrophoresis sample buffer, resolved in 10% or 12% mini SDS-PAGE, transferred to PVDF, and probed with indicated antibodies. Bands were visualized and intensities were measured with an Alpha Innotech FluorChemQ MultiImage III instrument. Molecular weight standards are indicated at left, and ratios of each protein (infected divided by mock-infected) are indicated for each protein at right. Protein ratios are an average of three experiments each from A549 cells and a single HBAE donor and are reported after normalization to GAPDH.

ISG15 and RSAD2, interferon-induced proteins with anti-influenza activity, were also up-regulated in A549 cells[21,22] and primary macrophages.[16,47] These proteins have also been identified in proteomics studies of human host cell responses to infection with other viruses such as RSV,[48] adenovirus,[49] and sindbis virus and HSV.[50] Interferon-induced tetratricopeptide repeat proteins (IFIT1−3) have also been found in multiple proteomic studies of influenza involving primary macrophages,[16] the polarized Calu-3 airway epithelial cell line[23] and animal models.[24−26] Interestingly, these three IFIT proteins have been discovered to form an antiviral complex against 5′-triphosphate RNA,[51] which is thought to be present during an influenza infection. It is likely that these similar responses to different types of infection reflect the induction of a nonspecific innate immune response against RNA viruses by the host cells.

Down-Regulated Processes

We found 19 proteins that were consistently and strongly down-regulated in primary HBAE cells in response to influenza infection, and these were mainly linked to cell adhesion, death receptor signaling, and lipid metabolism.

Cellular adhesion is necessary for the survival of primary cells, and previous studies have found that a reduction in adhesion molecules precedes and may possibly be instrumental in inducing cell death.[52] In epithelial cells adherens junction proteins are essential for cell adhesion and these are largely composed of integrin, cadherin, catenin, and actin complexes.[53] Many proteins belonging to these complexes and downstream signaling pathways were detected in our SILAC data among which integrin β 4 was down-regulated 2.4-fold, GLG1 2.5-fold, and THBS1 2.6-fold. Other adhesion-related proteins such as fibronectin, laminin, TGFBI, and TNC were down-regulated >2.0-fold.

However, cell death processes were not identified by any of our analyses, except for the down-regulation of two TRAIL receptors, TNFSFR10A and TNFSFR10B (Figures 4b and 5b). TNFRSF10A, TNFRSF10B and F3 are additionally associated with caspase activity induction, which was similarly indicated as down-regulated (Figure 4b). In contrast, TNFSFR10D was

found up-regulated 1.4-fold in PR8-infected A549 cells at the same time point.[22] Given that TRAIL signaling is important in clearing influenza-infected epithelial cells, it would be interesting to further investigate the mechanism by which TRAIL-receptors are down-regulated in HBAE.

As cholesterol and lipids are key to maintaining the integrity of the cell membrane and the organization of lipid rafts, it was interesting to find that several proteins related to lipid biosynthesis were down-regulated in response to influenza. For example, a previous study indicated that RSAD2 interferes with cholesterol synthesis and subsequent lipid raft integrity by binding and inhibiting FPPS, an enzyme in the cholesterol biosynthetic pathway.[54,55] Our SILAC/HBAE data found RSAD2 highly up-regulated (>3-fold) and FPPS moderately up-regulated (1.5-fold) (Supplementary Figure 1c). Importantly, FPPS is involved not only in the production of cholesterol but also other intermediates, such as isoprenoids FPP and GGPP, which serve as essential activators of GTPase proteins. Our SILAC data identified a number of proteins from this pathway, of which FDFT1 was most significantly altered (2.9-fold down-regulated). Fatty acid synthesis was also affected through a strong downregulation of FADS2 (3.45-fold). A second study has also found that interferon signaling can suppress sterol biosynthesis in macrophages,[56] suggesting that this may be a protective response induced by the host cell rather than by the virus. While none of FPPS, FDFT1, nor FADS2 were altered in A549 cells at 24 hpi, IPA indicated other lipid-related pathways as down-regulated in A549 cells including sphingolipid metabolism and VDR/RXR signaling. Collectively, these data suggest that lipid metabolism may be inhibited in epithelial cells during influenza infection.

■ CONCLUSION

Overall this proteomics study provides a broad and unbiased profile of cytoplasmic host cell proteins that are up- and down-regulated in response to an H1N1 mouse-adapted influenza virus in primary human airway epithelial cells. While some of our findings correlate with previous proteomic studies involving influenza or other viruses, we have identified many proteins that

have not been previously studied with respect to influenza. Thus, our work has expanded the knowledge base for understanding host cell response to influenza infection. Of note, we performed our studies using relevant primary human bronchial epithelial cells, whereas many previous studies have been conducted using transformed cell lines such as alveolar A549 cells or nonlung HEK293 cells. A comparison of functional categories and pathway alterations between our studies with A549 and HBAE identified some common characteristics such as downregulation of cell adhesion and lipid metabolism, as well as upregulation of host defense responses against influenza infection. In contrast, downregulation of TRAIL receptors was specific to HBAE cells. Further validation and investigation into the functions of the candidate proteins we have identified will contribute to understanding novel virus-host interactions and permit integration of this information with previous large-scale analyses of influenza to identify new directions for developing anti-influenza therapies.

■ ASSOCIATED CONTENT

ⓢ Supporting Information

This material is available free of charge via the Internet at http://pubs.acs.org.

■ AUTHOR INFORMATION

Corresponding Author

*Phone: 204.789.3976. Fax: 204.480.1362. E-mail: kcoombs@cc.umanitoba.ca.

Notes

The authors declare no competing financial interest.

■ ACKNOWLEDGMENTS

■ ABBREVIATIONS

HBAE, human bronchial airway epithelial cells; hpi, hours post infection; IAV, influenza A virus; INF, interferon; NS-1, nonstructural protein 1; PR8, influenza strain A/PR/8/34; SILAC, stable isotope labeling of amino acids in cell culture

■ REFERENCES

(1) Palese, P.; Shaw, M. L. Orthomyxoviridae: The Viruses and Their Replication. In *Fields Virology*, 5th ed.; Lippencott Williams & Wilkins: Philadelphia, 2007; Vol. 2, pp 1647−1689.

(2) Shapira, S. D.; Gat-Viks, I.; Shum, B. O.; Dricot, A.; de Grace, M. M.; Wu, L.; Gupta, P. B.; Hao, T.; Silver, S. J.; Root, D. E.; Hill, D. E.; Regev, A.; Hacohen, N. A physical and regulatory map of host-influenza interactions reveals pathways in H1N1 infection. *Cell* 2009, 139 (7), 1255−67.

(3) Kash, J. C.; Goodman, A. G.; Korth, M. J.; Katze, M. G. Hijacking of the host-cell response and translational control during influenza virus infection. *Virus Res.* 2006, 119 (1), 111−20.

(4) Gannage, M.; Dormann, D.; Albrecht, R.; Dengjel, J.; Torossi, T.; Ramer, P. C.; Lee, M.; Strowig, T.; Arrey, F.; Conenello, G.; Pypaert, M.; Andersen, J.; Garcia-Sastre, A.; Munz, C. Matrix protein 2 of influenza A virus blocks autophagosome fusion with lysosomes. *Cell Host Microbe* 2009, 6 (4), 367−80.

(5) Ludwig, S.; Pleschka, S.; Planz, O.; Wolff, T. Ringing the alarm bells: signalling and apoptosis in influenza virus infected cells. *Cell Microbiol.* 2006, 8 (3), 375−86.

(6) Sumbayev, V. V.; Yasinska, I. M. Role of MAP kinase-dependent apoptotic pathway in innate immune responses and viral infection. *Scand. J. Immunol.* 2006, 63 (6), 391−400.

(7) Hale, B. G.; Randall, R. E.; Ortin, J.; Jackson, D. The multifunctional NS1 protein of influenza A viruses. *J. Gen. Virol.* 2008, 89 (Pt 10), 2359−76.

(8) Hao, L.; Sakurai, A.; Watanabe, T.; Sorensen, E.; Nidom, C. A.; Newton, M. A.; Ahlquist, P.; Kawaoka, Y. Drosophila RNAi screen identifies host genes important for influenza virus replication. *Nature* 2008, 454 (7206), 890−3.

(9) Brass, A. L.; Huang, I. C.; Benita, Y.; John, S. P.; Krishnan, M. N.; Feeley, E. M.; Ryan, B. J.; Weyer, J. L.; van der Weyden, L.; Fikrig, E.; Adams, D. J.; Xavier, R. J.; Farzan, M.; Elledge, S. J. The IFITM proteins mediate cellular resistance to influenza A H1N1 virus, West Nile virus, and dengue virus. *Cell* 2009, 139 (7), 1243−54.

(10) Konig, R.; Stertz, S.; Zhou, Y.; Inoue, A.; Hoffmann, H. H.; Bhattacharyya, S.; Alamares, J. G.; Tscherne, D. M.; Ortigoza, M. B.; Liang, Y.; Gao, Q.; Andrews, S. E.; Bandyopadhyay, S.; De Jesus, P.; Tu, B. P.; Pache, L.; Shih, C.; Orth, A.; Bonamy, G.; Miraglia, L.; Ideker, T.; Garcia-Sastre, A.; Young, J. A.; Palese, P.; Shaw, M. L.; Chanda, S. K. Human host factors required for influenza virus replication. *Nature* 2010, 463 (7282), 813−7.

(11) Karlas, A.; Machuy, N.; Shin, Y.; Pleissner, K. P.; Artarini, A.; Heuer, D.; Becker, D.; Khalil, H.; Ogilvie, L. A.; Hess, S.; Maurer, A. P.; Muller, E.; Wolff, T.; Rudel, T.; Meyer, T. F. Genome-wide RNAi screen identifies human host factors crucial for influenza virus replication. *Nature* 2010, 463 (7282), 818−22.

(12) Ludwig, S. Targeting cell signalling pathways to fight the flu: towards a paradigm change in anti-influenza therapy. *J. Antimicrob. Chemother.* 2009, 64 (1), 1−4.

(13) Pathak, S.; De Souza, G. A.; Salte, T.; Wiker, H. G.; Asjo, B. HIV induces both a down-regulation of IRAK-4 that impairs TLR signalling and an up-regulation of the antibiotic peptide dermcidin in monocytic cells. *Scand. J. Immunol.* 2009, 70 (3), 264−76.

(14) Mannova, P.; Fang, R.; Wang, H.; Deng, B.; McIntosh, M. W.; Hanash, S. M.; Beretta, L. Modification of host lipid raft proteome upon hepatitis C virus replication. *Mol. Cell. Proteomics* 2006, 5 (12), 2319−25.

(15) Kang, S. M.; Shin, M. J.; Kim, J. H.; Oh, J. W. Proteomic profiling of cellular proteins interacting with the hepatitis C virus core protein. *Proteomics* 2005, 5 (8), 2227−37.

(16) Lietzen, N.; Ohman, T.; Rintahaka, J.; Julkunen, I.; Aittokallio, T.; Matikainen, S.; Nyman, T. A. Quantitative subcellular proteome and secretome profiling of influenza A virus-infected human primary macrophages. *PLoS Pathog.* 2011, 7 (5), e1001340.

(17) Ohman, T.; Rintahaka, J.; Kalkkinen, N.; Matikainen, S.; Nyman, T. A. Actin and RIG-I/MAVS signaling components translocate to mitochondria upon influenza A virus infection of human primary macrophages. *J. Immunol.* 2009, 182 (9), 5682−92.

(18) Liu, N.; Song, W.; Wang, P.; Lee, K.; Chan, W.; Chen, H.; Cai, Z. Proteomics analysis of differential expression of cellular proteins in response to avian H9N2 virus infection in human cells. *Proteomics* 2008, 8 (9), 1851−8.

(19) Zhang, L.; Zhang, X.; Ma, Q.; Ma, F.; Zhou, H. Transcriptomics and proteomics in the study of H1N1 2009. *Genomics, Proteomics Bioinf.* 2010, 8 (3), 139−44.

(20) Vester, D.; Rapp, E.; Gade, D.; Genzel, Y.; Reichl, U. Quantitative analysis of cellular proteome alterations in human influenza A virus-infected mammalian cell lines. *Proteomics* **2009**, *9* (12), 3316−27.

(21) Liu, H. C.; Hicks, J.; Yoo, D. Proteomic dissection of viral pathogenesis. *Dev. Biol. (Basel)* **2008**, *132*, 43−53.

(22) Coombs, K. M.; Berard, A.; Xu, W.; Krokhin, O.; Meng, X.; Cortens, J. P.; Kobasa, D.; Wilkins, J.; Brown, E. G. Quantitative proteomic analyses of influenza virus-infected cultured human lung cells. *J. Virol.* **2010**, *84* (20), 10888−906.

(23) Li, C.; Bankhead, A.; Eisfeld, A. J.; Hatta, Y.; Jeng, S.; Chang, J. H.; Aicher, L. D.; Proll, S.; Ellis, A. L.; Law, G. L.; Waters, K.; Neumann, G.; Katze, M. G.; McWeeney, S.; Kawaoka, Y. Host regulatory network response to infection with highly pathogenic H5N1 avian influenza virus. *J. Virol.* **2011**, *85*, 10955−67.

(24) Zinman, G.; Brower-Sinning, R.; Emeche, C. H.; Ernst, J.; Huang, G. T.; Mahony, S.; Myers, A. J.; O'Dee, D. M.; Flynn, J. L.; Nau, G. J.; Ross, T. M.; Salter, R. D.; Benos, P. V.; Bar Joseph, Z.; Morel, P. A. Large scale comparison of innate responses to viral and bacterial pathogens in mouse and macaque. *PLoS One* **2011**, *6* (7), e22401.

(25) Brown, J. N.; Palermo, R. E.; Baskin, C. R.; Gritsenko, M.; Sabourin, P. J.; Long, J. P.; Sabourin, C. L.; Bielefeldt-Ohmann, H.; Garcia-Sastre, A.; Albrecht, R.; Tumpey, T. M.; Jacobs, J. M.; Smith, R. D.; Katze, M. G. Macaque proteome response to highly pathogenic avian influenza and 1918 reassortant influenza virus infections. *J. Virol.* **2010**, *84* (22), 12058−68.

(26) Baas, T.; Baskin, C. R.; Diamond, D. L.; Garcia-Sastre, A.; Bielefeldt-Ohmann, H.; Tumpey, T. M.; Thomas, M. J.; Carter, V. S.; Teal, T. H.; Van Hoeven, N.; Proll, S.; Jacobs, J. M.; Caldwell, Z. R.; Gritsenko, M. A.; Hukkanen, R. R.; Camp, D. G., 2nd; Smith, R. D.; Katze, M. G. Integrated molecular signature of disease: analysis of influenza virus-infected macaques through functional genomics and proteomics. *J. Virol.* **2006**, *80* (21), 10813−28.

(27) Scull, M. A.; Gillim-Ross, L.; Santos, C.; Roberts, K. L.; Bordonali, E.; Subbarao, K.; Barclay, W. S.; Pickles, R. J. Avian Influenza virus glycoproteins restrict virus replication and spread through human airway epithelium at temperatures of the proximal airways. *PLoS Pathog.* **2009**, *5* (5), e1000424.

(28) Ibricevic, A.; Pekosz, A.; Walter, M. J.; Newby, C.; Battaile, J. T.; Brown, E. G.; Holtzman, M. J.; Brody, S. L. Influenza virus receptor specificity and cell tropism in mouse and human airway epithelial cells. *J. Virol.* **2006**, *80* (15), 7469−80.

(29) Chan, R. W.; Yuen, K. M.; Yu, W. C.; Ho, C. C.; Nicholls, J. M.; Peiris, J. S.; Chan, M. C. Influenza H5N1 and H1N1 virus replication and innate immune responses in bronchial epithelial cells are influenced by the state of differentiation. *PLoS One* **2010**, *5* (1), e8713.

(30) Thompson, C. I.; Barclay, W. S.; Zambon, M. C.; Pickles, R. J. Infection of human airway epithelium by human and avian strains of influenza a virus. *J. Virol.* **2006**, *80* (16), 8060−8.

(31) Spicer, V.; Yamchuk, A.; Cortens, J.; Sousa, S.; Ens, W.; Standing, K. G.; Wilkins, J. A.; Krokhin, O. V. Sequence-specific retention calculator. A family of peptide retention time prediction algorithms in reversed-phase HPLC: applicability to various chromatographic conditions and columns. *Anal. Chem.* **2007**, *79* (22), 8762−8.

(32) Dwivedi, R. C.; Spicer, V.; Harder, M.; Antonovici, M.; Ens, W.; Standing, K. G.; Wilkins, J. A.; Krokhin, O. V. Practical implementation of 2D HPLC scheme with accurate peptide retention prediction in both dimensions for high-throughput bottom-up proteomics. *Anal. Chem.* **2008**, *80* (18), 7036−42.

(33) Ho, Y. S.; Wang, Y. J.; Lin, J. K. Induction of p53 and p21/WAF1/CIP1 expression by nitric oxide and their association with apoptosis in human cancer cells. *Mol. Carcinog.* **1996**, *16* (1), 20−31.

(34) Huang da, W.; Sherman, B. T.; Lempicki, R. A. Systematic and integrative analysis of large gene lists using DAVID bioinformatics resources. *Nat. Protoc.* **2009**, *4* (1), 44−57.

(35) Dennis, G., Jr.; Sherman, B. T.; Hosack, D. A.; Yang, J.; Gao, W.; Lane, H. C.; Lempicki, R. A. DAVID: Database for annotation, visualization, and integrated discovery. *Genome Biol.* **2003**, *4* (5), P3.

(36) Abedin, M. J.; Wang, D.; McDonnell, M. A.; Lehmann, U.; Kelekar, A. Autophagy delays apoptotic death in breast cancer cells following DNA damage. *Cell Death Differ.* **2007**, *14* (3), 500−10.

(37) Arcangeletti, M. C.; De Conto, F.; Ferraglia, F.; Pinardi, F.; Gatti, R.; Orlandini, G.; Covan, S.; Motta, F.; Rodighiero, I.; Dettori, G.; Chezzi, C. Host-cell-dependent role of actin cytoskeleton during the replication of a human strain of influenza A virus. *Arch. Virol.* **2008**, *153* (7), 1209−21.

(38) Arumugam, E.; Pereira, J.; Gilbert, P. M. Reconstruction after skin sparing mastectomy. *Ann. R. Coll. Surg. Engl.* **2005**, *87* (4), 314 ; author reply 314.

(39) Hsu, A. C.; Barr, I.; Hansbro, P. M.; Wark, P. A. Human Influenza is More Effective than Avian Influenza at Antiviral Suppression in Airway Cells. *Am. J. Respir. Cell Mol. Biol.* **2010**, *44*, 906−13.

(40) Trapp, S.; Derby, N. R.; Singer, R.; Shaw, A.; Williams, V. G.; Turville, S. G.; Bess, J. W., Jr.; Lifson, J. D.; Robbiani, M. Double-stranded RNA analog poly(I:C) inhibits human immunodeficiency virus amplification in dendritic cells via type I interferon-mediated activation of APOBEC3G. *J. Virol.* **2009**, *83* (2), 884−95.

(41) Murphy, J. A.; Duerst, R. J.; Smith, T. J.; Morrison, L. A. Herpes simplex virus type 2 virion host shutoff protein regulates alpha/beta interferon but not adaptive immune responses during primary infection in vivo. *J. Virol.* **2003**, *77* (17), 9337−45.

(42) Yu, F. F.; Zhang, Y. B.; Liu, T. K.; Liu, Y.; Sun, F.; Jiang, J.; Gui, J. F. Fish virus-induced interferon exerts antiviral function through Stat1 pathway. *Mol. Immunol.* **2010**, *47* (14), 2330−41.

(43) Haye, K.; Burmakina, S.; Moran, T.; Garcia-Sastre, A.; Fernandez-Sesma, A. The NS1 protein of a human influenza virus inhibits type I interferon production and the induction of antiviral responses in primary human dendritic and respiratory epithelial cells. *J. Virol.* **2009**, *83* (13), 6849−62.

(44) Mibayashi, M.; Martinez-Sobrido, L.; Loo, Y. M.; Cardenas, W. B.; Gale, M., Jr.; Garcia-Sastre, A. Inhibition of retinoic acid-inducible gene I-mediated induction of beta interferon by the NS1 protein of influenza A virus. *J. Virol.* **2007**, *81* (2), 514−24.

(45) Hale, B. G.; Barclay, W. S.; Randall, R. E.; Russell, R. J. Structure of an avian influenza A virus NS1 protein effector domain. *Virology* **2008**, *378* (1), 1−5.

(46) Geiss, G. K.; Salvatore, M.; Tumpey, T. M.; Carter, V. S.; Wang, X.; Basler, C. F.; Taubenberger, J. K.; Bumgarner, R. E.; Palese, P.; Katze, M. G.; Garcia-Sastre, A. Cellular transcriptional profiling in influenza A virus-infected lung epithelial cells: the role of the nonstructural NS1 protein in the evasion of the host innate defense and its potential contribution to pandemic influenza. *Proc. Natl. Acad. Sci. U.S.A.* **2002**, *99* (16), 10736−41.

(47) Lee, S. M.; Gardy, J. L.; Cheung, C. Y.; Cheung, T. K.; Hui, K. P.; Ip, N. Y.; Guan, Y.; Hancock, R. E.; Peiris, J. S. Systems-level comparison of host-responses elicited by avian H5N1 and seasonal H1N1 influenza viruses in primary human macrophages. *PLoS One* **2009**, *4* (12), e8072.

(48) Munday, D.; Emmott, E.; Surtees, R.; Lardeau, C. H.; Wu, W.; Duprex, W. P.; Dove, B. K.; Barr, J. N.; Hiscox, J. A. Quantitative proteomic analysis of A549 cells infected with human respiratory syncytial virus. *Mol. Cell. Proteomics* **2010**, *9*, 2438−59.

(49) Zhao, H.; Boije, H.; Granberg, F.; Pettersson, U.; Svensson, C. Activation of the interferon-induced STAT pathway during an adenovirus type 12 infection. *Virology* **2009**, *392* (2), 186−95.

(50) Lenschow, D. J.; Lai, C.; Frias-Staheli, N.; Giannakopoulos, N. V.; Lutz, A.; Wolff, T.; Osiak, A.; Levine, B.; Schmidt, R. E.; Garcia-Sastre, A.; Leib, D. A.; Pekosz, A.; Knobeloch, K. P.; Horak, I.; Virgin, H. W. t. IFN-stimulated gene 15 functions as a critical antiviral molecule against influenza, herpes, and Sindbis viruses. *Proc. Natl. Acad. Sci. U.S.A.* **2007**, *104* (4), 1371−6.

(51) Pichlmair, A.; Lassnig, C.; Eberle, C. A.; Gorna, M. W.; Baumann, C. L.; Burkard, T. R.; Burckstummer, T.; Stefanovic, A.; Krieger, S.; Bennett, K. L.; Rulicke, T.; Weber, F.; Colinge, J.; Muller, M.; Superti-Furga, G. IFIT1 is an antiviral protein that recognizes 5′-triphosphate RNA. *Nat. Immunol.* **2011**, *12* (7), 624−30.

(52) Ling, Y.; Zhong, Y.; Perez-Soler, R. Disruption of cell adhesion and caspase-mediated proteolysis of beta- and gamma-catenins and APC

protein in paclitaxel-induced apoptosis. *Mol. Pharmacol.* **2001**, *59* (3), 593−603.

(53) Suzanne, M.; Steller, H. Letting go: modification of cell adhesion during apoptosis. *J. Biol.* **2009**, *8* (5), 49.

(54) Wang, X.; Hinson, E. R.; Cresswell, P. The interferon-inducible protein viperin inhibits influenza virus release by perturbing lipid rafts. *Cell Host Microbe* **2007**, *2* (2), 96−105.

(55) Waheed, A. A.; Freed, E. O. Influenza virus not cRAFTy enough to dodge viperin. *Cell Host Microbe* **2007**, *2* (2), 71−2.

(56) Blanc, M.; Hsieh, W. Y.; Robertson, K. A.; Watterson, S.; Shui, G.; Lacaze, P.; Khondoker, M.; Dickinson, P.; Sing, G.; Rodriguez-Martin, S.; Phelan, P.; Forster, T.; Strobl, B.; Muller, M.; Riemersma, R.; Osborne, T.; Wenk, M. R.; Angulo, A.; Ghazal, P. Host defense against viral infection involves interferon mediated down-regulation of sterol biosynthesis. *PLoS Biol.* **2011**, *9* (3), e1000598.